

Theoretical Design of High-Spin Polycyclic Hydrocarbons

Georges Trinquier, Nicolas Suaud, and Jean-Paul Malrieu*^[a]

Abstract: High-spin organic structures can be obtained from fused polycyclic hydrocarbons, by converting selected peripheral HC(sp²) sites into H₂C(sp³) ones, guided by Ovchinnikov's rule. Theoretical investigation is performed on a few examples of such systems, involving three to twelve fused rings, and maintaining threefold symmetry. Unrestricted DFT (UDFT) calculations, including geometry optimizations, confirm the high-spin multiplicity of the ground state. Spin-density distributions and low-energy spectra are further

studied through geometry-dependent Heisenberg–Hamiltonian diagonalizations and explicit correlated ab initio treatments, which all agree on the high-spin character of the suggested structures, and locate the low-lying states at significantly higher energies. In particular, the lowest-lying state of

lower multiplicity is always found to be higher than kT at room temperature (at least ten times higher). Simplification of the ferromagnetic organization based on sets of semilocalized non-bonding orbitals is proposed. Molecular architectures are thus conceived in which the ferromagnetically-coupled unpaired electrons tally up to one third of the involved conjugated carbons. Connecting such building blocks should provide bidimensional materials endowed with robust magnetic properties.

Keywords: density functional calculations · high-spin polycyclic hydrocarbons · magnetic properties · Ovchinnikov's rule

Introduction

Magnetic properties of materials have received intense attention, both as an intellectually challenging problem, and for their technical potentialities. Ferromagnetism was initially the privilege of metallic lattices or metal oxides until coordination chemistry provided molecular complexes with paramagnetic ground states, and the possibility of high-spin multiplicity.^[1–5] Later on, the possibility to arrange these complexes into 1D, 2D, or 3D lattices with ferromagnetic or ferrimagnetic order has been investigated and achieved.^[6–8] Magnetic materials involving metallic centers, as spin carriers, present fascinating properties: High- T_c superconductors are obtained by doping spin lattices;^[9–12] other systems exhibit colossal magneto-resistance.^[13–15] Lattices of organometallic complexes, such as Prussian-blue analogs, present bistability with hysteresis, and offer the possibility to behave as information bits.^[16] Similar properties may be obtained at

the molecular or cluster scale as in single-molecule magnets.^[17,18] The question we would like to raise from the present work and forthcoming ones concerns the possibility to conceive metal-atom free, purely organic analogues of these materials.

The conception of high-spin organic molecules has a rather long history and contains significant successes. The most popular stable organic radicals are the nitroxide radicals, and tentative ferromagnetic couplings of polyradicals of this type have been proposed.^[19–20] With pure conjugated hydrocarbons, one strategy consists in coupling either triplet ground-state carbenes or -CH- sites through conjugated bridges, such as *meta*-connected benzene rings (note that *meta*-xylene has a triplet ground state).^[21–23] On these grounds, Rajca et al. conceived, synthesized, and characterized ferromagnetic assemblies of one-half spin free radicals that achieve quite sizeable total moments.^[24–30] Although most of these molecular architectures are dendrimeric and have limited sizes, these authors have opened a rather fascinating domain, encompassing spintronics and nonlinear optical responses.^[31]

The present work proposes organic paramagnetic molecules with both a high-multiplicity ground state and high-spin nuclearity, or high density of ferromagnetically coupled unpaired electrons—one unpaired electron for three conjugated carbon atoms.^[32] Rather than being polyradicals with

[a] Dr. G. Trinquier, Dr. N. Suaud, Dr. J.-P. Malrieu
Laboratoire de Chimie et Physique Quantiques
(CNRS, UMR-5626), IRSAMC
Université Paul-Sabatier, 31062 Toulouse Cedex (France)
E-mail: trinquier@irsamc.ups-tlse.fr

unpaired electrons located on well-identified sites, these molecular systems all exhibit several parallel spins on the *same* conjugated frame, without possible localization in definite and separated regions.

The principle of this conception is presented below. It is based on the vision of π electrons, as an assembly of spins, ruled by a Heisenberg–Hamiltonian with inter-site antiferromagnetic coupling. Starting from fused aromatic hydrocarbons with a singlet or doublet ground state, high total-spin multiplicity is created or enhanced by changing the hybridization of appropriate peripheral carbons from sp^2 into sp^3 , that is, by changing selected peripheral CH groups into CH_2 groups. The qualitative predictions are put to the test by using computations at both *ab initio* level and by using semi-empirical Hamiltonians. Ground-state spin multiplicities, spin densities, and vertical transition energies to states of lower spin multiplicity are also addressed. Moreover, we discuss these results and outline the strategy to be followed in conceiving ferromagnetic assemblies of the proposed organic units, which will be the objective of forthcoming work.

Qualitative conception from fused polyaromatic molecules

Ovchinnikov's rule and the coloring problem: The π -electron population of a conjugated hydrocarbon can be seen as an assembly of $S=1/2$ spins. This sounds paradoxical, as these populations are usually considered to be highly delocalized (a nearly metallic half-filled band system), however the magnetic descriptions are estimated to be relevant only in strong-correlation limits for which the electronic repulsion is large and severely restricts the fluctuation of the electronic population close to its mean value—in our case one π -electron per carbon. When this is valid, the leading valence-bond (VB) space configuration is the neutral one. Playing only with the spin distributions on different sites, the possible antiferromagnetic (AF) spin exchanges between adjacent spin carriers come from weak delocalization effects, which introduce some influence on ionic VB structures that are coupled with different neutral spin distributions.

We therefore face two models for half-filled bands. One is the independent-particle approximation, as encountered in the Hückel picture, the Hartree–Fock method, or the Kohn–Sham version of the density functional theory (DFT). The other one is the Heisenberg Hamiltonian, which only considers on-site spins. The domains of applicability of these models are not mutually exclusive, because a same system of electrons can be treated from both entries, as illustrated in conjugated hydrocarbons.

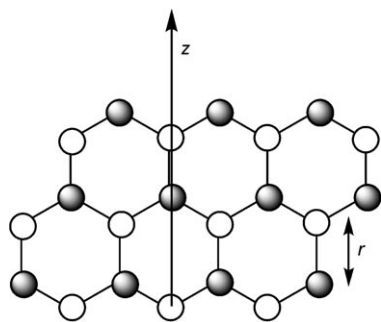
In these systems, the ratio of the absolute value of the hopping integral t , moving the electrons from one site to its adjacent one, to the effective on-site repulsion U , that is, the energy difference between neutral and ionic VB structures, is around 0.7, which pushes them preferably to the strong-delocalization side. Nevertheless, the magnetic description proved to be relevant and able to furnish qualitative and quantitative information.^[33–35] A geometry-dependent Heisenberg Hamiltonian has been developed from *ab initio* cal-

culations on the ground state and the low-lying triplet state of ethylene.^[36] Applied to conjugated hydrocarbons, it proved capable of predicting ground-state and excited-state geometries, energies, and rotational barriers.^[37] Under the label MMVB (molecular mechanics with valence-bond), the model has been extensively exploited by Robb et al. on photochemical processes of conjugated hydrocarbons.^[38–44]

A qualitative consequence of this magnetic view is the possibility to predict ground-state spin multiplicities. As inter-site exchange is antiferromagnetic, the lowest-energy spin distribution avoids, as much as possible, spin frustrations between adjacent sites. The determinant of lowest energy, associated to the largest coefficient in the ground-state wavefunction, is the one in which each atom bearing an α spin is surrounded by adjacent β spins, and reciprocally. This distribution offers the possibility for inter-site delocalization through electron hopping on each chemical bond (spin exchange), whereas no delocalization can occur between two parallel spins located on adjacent atoms, owing to the Pauli principle. A distribution insuring spin alternation on all bonds is always possible, except when odd-membered rings are present in the molecular graph. All other systems, open chains, branched systems, four- and six-membered rings and their combinations, are called “alternant” by chemists, and “bipartite” by physicists. A coloring feature characterizes them, associating a given color to any starting atom, then a different color on its first neighbors and so on, two atoms of the same color are never first neighbors—the definition of a chromatic index of two.

The most-alternant spin distribution does not necessarily correspond to $M_s=0$ (even number of sites), or $M_s=1/2$ (odd number of sites), and may exhibit more α than β , as illustrated below. As it is energetically favored, Ovchinnikov has speculated that the ground-state total spin is given by the difference between the number of sites of different colors ($S=1/2 |N_a-N_b|$), resulting in a spin-multiplicities singlet when $N_a=N_b$, a doublet when $N_a=N_b+1$, a triplet when $N_a=N_b+2$, and so on.^[45,46] As far as planar alternant conjugated hydrocarbons are concerned, there is no counterexample to this rule.^[47] For non-alternant frames, its exploitation may turn ambiguous, in a context of singlet–triplet bistability.^[48,49]

Application to fused polyaromatic hydrocarbons: Benzene, naphthalene, anthracene, and larger polyacenes have a singlet ground state for which $N_a=N_b$. The nature of the ground state does not change if a second rank of hexagons is added to the first one, keeping a same number of hexagons in the two ranks, and any number of superposed ranks. Taking a z axis perpendicular to the ranks, the z coordinate of the atoms will be 0, $r/2$, $3r/2$, $2r$, $(2+1/2)r$ and so on (see Scheme 1), the atoms of a same z keeping the same color, and colors changing between closest z . To create unbalance between N_a and N_b , different ranks of hexagons must have different lengths. This can be fulfilled by adding an hexagon on top of naphthalene, giving the phenalene radical (**1a** in Scheme 2),^[50] characterized by its D_{3h} symmetry, odd



Scheme 1.

number of carbons, and doublet spin multiplicity, as $N_a = N_b + 1$.

In turn, a larger compound of regular triangular shape can be built by adding the previous free radical on top of anthracene, **2a**. As $N_a = N_b + 2$, one may expect here a triplet ground state for a total of 22 conjugated carbons. The next triangular architecture, **3a**, would superpose four ranks, with expected quartet ground state since $N_a = N_b + 3$. One may go on and increase the ground-state spin multiplicity by adding one unpaired electron at each step. In this way, $N_a - N_b$ is equal to the number of superposed ranks minus one, but the density of parallel electrons, $(N_a - N_b)/(N_a + N_b)$, remains low, decreasing as the inverse of the number of conjugated atoms. These architectures differ from usual polyradicals in that there is no precise localization of the unpaired electrons, they coexist over delocalized regions and cannot be attributed to precise sites. Regardless of the equivalent Lewis depiction, Kekulé structures always leave $(N_a - N_b)$ atoms outside the double bonds.

Except at the corners, all peripheral atoms have the dominant color. As corner atoms have the minor color, changing their nature by transforming them into sp^3 carbons (by adding one hydrogen or halogen), or subtracting them from the conjugated system will lead to significantly higher spin, as $(N_a - N_b)$ is increased by 3. Scheme 2 illustrates the obtained molecular structures for two, three, and four superposed ranks of hexagons. For the smaller system, **1**, the expected ground-state multiplicity is a quintet, corresponding to four parallel spins on ten conjugated carbons, to result in a density of unpaired electrons of $(N_a - N_b)/(N_a + N_b) = 2/5$. This density decreases when increasing the size of the system, as illustrated by the sextet ground state of **2**, for which five unpaired electrons of parallel spins spread over 19 conjugated carbons, leading to a density of 5/19.

In a context of selective polyaromatic reductions,^[51–56] these ideas should not be limited to the above series. Restricting ourselves to D_{3h} symmetries, let us consider coronene **4a**. Saturating six peripheral atoms at appropriate positions will transform it into an hexa-substituted benzene **4**, which has a septet ground state in which six unpaired electrons of the same color spread on 18 conjugated carbons, conferring a density of parallel spins as high as 1/3.

An alternative view to this building strategy consists in first starting from aromatic or polyaromatic systems bearing exocyclic methylene groups at positions known to confer high-spin character. Then the hindrance, owing to two C–H bonds belonging to nearby radiating methylenes, is relieved by fusing these two hydrogens into a bridging methylene group $-CH_2-$. In this way, the high-spin property of the starting system is preserved, whatever its alteration in size and shape, as illustrated in the left part of Scheme 2. From this perspective, **4** derives from the fully-conjugated subgraph **4b**, whereas **5b**, the superior analog of **2b**, gives system **5** an octet ground state and bears seven unpaired electrons.

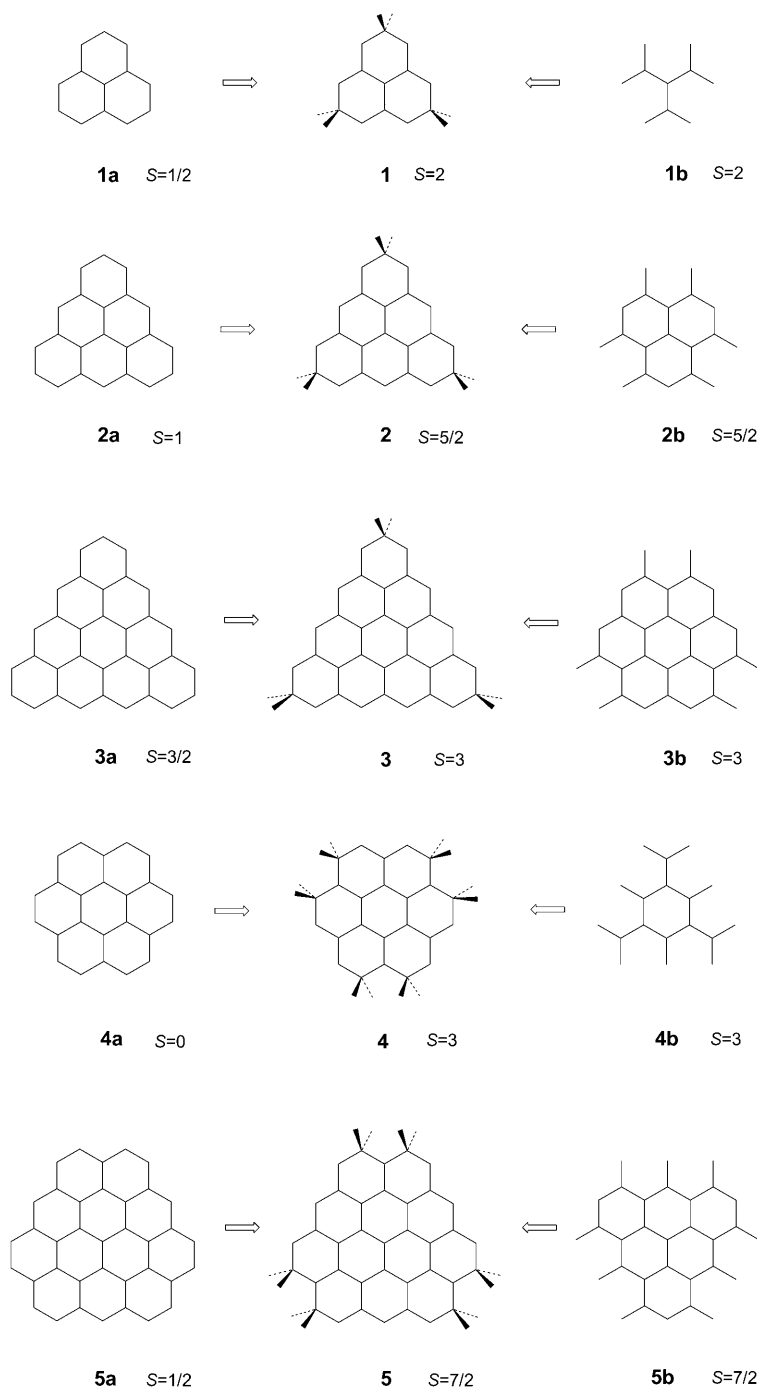
Naïve Hückel point of view: In such regular architectures one may expect that the polyradical character will naturally emerge from degenerate levels of zero energy in a Hückel treatment. Their number is equal to the number of unpaired electrons predicted by Ovchinnikov's rule. This is numerically checked by diagonalizing the topological Hamiltonian, but the correct number of orthogonal molecular orbitals (MOs)—the eigenvectors associated to zero eigenenergy—may be produced straightforwardly as well (see Polycyclic candidates with threefold symmetry). These eigenvectors may be semilocalized through a unitary transform of the symmetry-adapted ones and furnish an interesting view of the distribution of unpaired electrons. By using the eigenequation $(H - E)\phi = 0$, which becomes $H\phi = 0$, any orbital cancelled by the action of H is a nonbonding eigenvector. Acting on a given orbital, the Hamiltonian sends the amplitude C_i on atom i to adjacent atoms j with an amplitude t (or β). For the given atom i , the eigenequation requires a zero value for the sum of coefficients on adjacent atoms j [Eq. (1)]:

$$\sum_{j \text{ adj. to } i} C_j = 0 \quad (1)$$

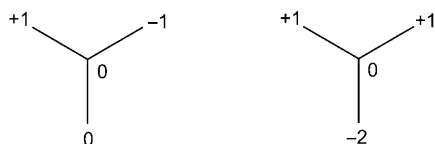
This is satisfied when all minor-color atoms have zero amplitudes and are surrounded by two major-color atoms of opposite amplitudes, as in allyl radical in which the orbital that has $+/0/-$ amplitudes along the frame satisfies the above equation. The same is true with the singly-occupied orbitals responsible for the triplet ground state of trimethylene-methane, as illustrated in Scheme 3 (but for normalization).

Because the above statements keep qualitative and speculative character, they need to be confirmed by wavefunctions or DFT calculations.

Before doing it, let's clarify a point we will rely on, later in this work. As developed in textbooks on magnetism,^[2] a set of two unpaired electrons in two localized orbitals ϕ_i and ϕ_j undergoes two essential effects: i) a direct exchange K_{ij} , positive, ferromagnetic, significant only if the orbitals have non-negligible amplitudes in the same region of space, and ii) an effective exchange, called "kinetic exchange", of opposite sign, antiferromagnetic, originating in the possible delocalization of electrons over the two sites, providing they



Scheme 2. Convergent strategies for building high-spin hydrocarbons.



Scheme 3.

have different spins. This contribution is proportional to the square of the integral $\langle \phi_i | H | \phi_j \rangle$ (H is for this instance

the Fock operator). When this integral is zero, the coupling is ferromagnetic, as in the present cases for which our semilocalized nonbonding orbitals are eigenfunctions of the Hückel or Fock mono-electronic Hamiltonian. Evaluation of the former direct exchange integrals K_{ij} from coefficients of nonbonding orbitals is straightforward, as long as the bi-electronic Hamiltonian is assumed to be of the Hubbard-type, that is, reduced to on-site repulsion integrals U . This is completed in the Appendix for compounds **1**, **2**, and **4**.

Numerical methods

Beyond Hückel calculations, which merely give the number of nonbonding orbitals, one should endeavor to assess ground-state multiplicities and excitation energies to the lowest states of different multiplicities. The most rigorous procedure handles the exact Hamiltonian and non-minimal basis sets. Since the states in competition are of open-shell character, it is necessary to start with a complete active space (CAS) dealing with the expected number of unpaired electrons in the same number of MOs. These orbitals can be obtained by a CASSCF calculation of the highest-spin multiplet. Then, diagonalization of the corresponding CI matrix gives a first evaluation of energy spacing between states of different multiplicities (CASCI calculations). As dynamical correlation may play a significant role in the amplitudes of these spacings, a post CASSCF calculation using sufficiently large basis sets is next required.^[57] Different methods are available to this end. In the CASPT2 method, all the simple and double perturbations are taken into account in a second-order perturbative way.^[58] The difference-dedicated CI method (DDCI), a CAS-SDCI method that discards the purely inactive double excitations, can be considered as the most reliable method for estimating energy transitions in systems of chemical interest at reasonable expense.^[59] Two spaces of smaller size

are also used, namely CAS+S (including CAS and all single excitations to it) and DDCl2 (including CAS+S and two-electron excitations from closed-shell orbitals to active space ones, and from active-space orbitals to unoccupied ones). All these calculations provide true-spin eigenfunctions, but do not achieve geometry optimizations.

Density functional theory (DFT) calculations, on another hand, are efficient for geometry optimization. For the presently-considered systems, geometry optimizations have been performed on high-spin states, treated by an unrestricted DFT (UDFT) process.^[60] The expected maximum S_z value is kept in these computations, which of course suffer from some spin contamination, owing to the spin polarization of the supposedly closed-shell MOs. Nevertheless, mean values of the S^2 operator indicate that spin contamination remains moderate. The states of lower S_z are intrinsically multideterminantal and as such they are not directly accessible in Kohn–Sham formalism. A common practice in this domain is to perform broken spin-symmetry single-determinant calculations.^[61] If the system is to bear n open shells or unpaired electrons, one calculates first the solution corresponding to $S_{z\max}=n/2$. Starting from the MOs of this highest S_z solution, one may reverse the spin of one or two singly-occupied MOs, and optimize the energy for this new spin distribution. The so-obtained energy is usually assigned to that of an Ising Hamiltonian, that is, the diagonal energy of a Heisenberg Hamiltonian. The energy difference between the high-spin solution and these low- S_z solutions lead to the effective exchange between unpaired electrons. Back to the Heisenberg Hamiltonian, these quantities can be used to estimate the true spectrum of the system.

Being easy to use, this technique is frequently employed for systems in which unpaired electrons are located on different sites or regions of space. It becomes more ambiguous when the unpaired electrons are delocalized over a same region of space. In this case, the corresponding exchange integrals have no reason to be equal, and their amplitudes are not easy to obtain. Actually, in what follows, UDFT energies for $S_z < S_{z\max}$ are only reported as rough estimates for the vertical gaps between ground states and states of lower spin multiplicity. As shown below, if spin contamination remains weak for high-spin ground states for which $\langle S_{\text{GS}}^2 \rangle \approx 1/2 S(S+1)$, this is no longer true for solutions of lower S_z . For the first excited states, assuming spin contamination only originates from ground-state components, it is possible to estimate the excitation energy ΔE by exploiting the deviation of the mean value of S^2 operator for UHF (or UDFT) solutions $\langle S_{\text{UHF}}^2 \rangle$ with respect to its expected pure-spin excited-state value $\langle S_{\text{exc}}^2 \rangle$, through the relationship in Equation (2):

$$\langle S_{\text{UHF}}^2 \rangle = \lambda^2 \langle S_{\text{exc}}^2 \rangle + (1 - \lambda^2) \langle S_{\text{GS}}^2 \rangle \quad (2)$$

which leads through Equation (3):

$$\Delta E = \frac{\Delta E_{\text{UHF}}}{\lambda^2} \quad (3)$$

to Equation (4):

$$\Delta E = \Delta E_{\text{UHF}} \frac{\langle S_{\text{GS}}^2 \rangle - \langle S_{\text{exc}}^2 \rangle}{\langle S_{\text{GS}}^2 \rangle - \langle S_{\text{UHF}}^2 \rangle} \quad (4)$$

Incidentally, singlet–triplet energy differences in simple diradicals are known to strongly depend on the chosen density functional. For instance, in d^9 copper complexes,^[62] the B3LYP exchange–correlation potential may overestimate this energy gap by a factor of 1.5 to 2. As this ratio is not universal, the reliability of UB3LYP calculations has been tested on two typical organic biradicals. For trimethylene-methane, the UDFT approach gives a vertical (adiabatic) singlet–triplet separation of 1.10 eV (0.99 eV), to be compared with the accurate ab initio result of 1.18 eV (0.94 eV)^[63] and the experimental value of 0.79 eV.^[64] In *meta*-xylylene, our S – T energy difference is calculated at 0.61 eV (0.57 eV), to be compared with ab initio values of 0.60 eV (0.49 eV)^[65] and experimental adiabatic value of 0.42 eV.^[66] Apparently B3LYP, therefore, does not overestimate the magnetic coupling in organic diradicals, as it does in transition-metal complexes.

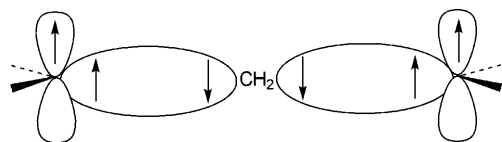
An alternative way to address the problem and estimate the low-energy spectrum is by using a Heisenberg Hamiltonian. A geometry-dependent Hamiltonian of this type has been proposed in which the σ system is treated through a sum of bond potentials R_{ij} , and the interaction between π electrons is expressed in terms of bicentric antiferromagnetic exchanges J_{ij} between sp^2 atoms.^[36] Summing over the pairs of linked atoms in Equation (5) with all π electrons being treated equally, gives:

$$H = \sum_{\text{linked } i,j} 2J_{ij}(\hat{S}_i \cdot \hat{S}_j - 1/4) + R_{ij} \quad (5)$$

The size of the vector space in which this Hamiltonian is developed is C_{2n}^n for a system involving $2n$ conjugated carbons, so that diagonalization is easy up to 24 sites. One might perform a geometry optimization for each state in this formalism, or use the UDFT optimized geometry for the ground state and calculate the vertical spectrum. A qualitative answer is given when taking a uniform value of the inter-atomic exchange integral, taken for the distance of 1.40 Å, namely 1 eV.

If two sp^2 -carbon atoms are bridged through a $-CH_2-$ methylene group, some interaction between them might be taken into account. Actually, calculations of the magnetic coupling between the remote unpaired electrons in $\dot{C}H_2-CH_2-\dot{C}H_2$ point to a rather low ferromagnetic value around 0.02 eV. This weak amplitude is owed to cancellation effects between anti-ferromagnetic delocalization originating in hyperconjugation, and ferromagnetic spin polarization along the σ skeleton, favoring Hund's rule at each carbon center (Scheme 4).

Among the above methods, the strict ab initio CI calculation is the most rigorous, as it uses the exact electronic Hamiltonian, provides eigenstates of S^2 , and may give posi-



Scheme 4.

tive and negative local spin densities. UDFT calculations also provide negative atomic spin densities, as they incorporate spin polarization, but the spectrum is here barely accessible. Advantages of this method are its low computational cost and its efficiency for geometry optimization. The Heisenberg Hamiltonian, on the other hand, gives estimates of energy separations at low cost, and positive/negative spin densities. Last, the Hückel Hamiltonian provides a qualitative entrance to the problem and gives the singly occupied MOs with their spatial localization, but cannot furnish on-site negative spin densities.

Polycyclic candidates with threefold symmetry

Calculated energies, geometries and spin densities are gathered in Tables 1–3, respectively, with corresponding labeling defined in Scheme 5.

Three-ring structures: The fully-conjugated structure **1a** is the well-known phenalenyl free radical.^[50] It is easy to see that its nonbonding MO is peripheral, with zero amplitude on the minor color sites and on the central atom, as illustrated from Hückel, UDFT and correlated ab initio spin densities reported in Table 3. Note that Heisenberg spin densities do not quite support this view, locating in this case a rather large density on central atom 2 (this originates in that Heisenberg treatment works with neutral forms only). As mentioned, saturating the three corners of **1a** produces **1**, a conjugated system of tri-allyl-methane type, kept planar by the CH₂ saturated groups connecting the allyl fragments, with a ground state corresponding to $S=2$. Of the four nonbonding

Table 2. UDFT-calculated bond lengths (in Å, see Scheme 5 for labeling).

Definitions	Values	Definitions	Values		
	1a	1	4a	4	
2–3	1.429	1.448	2–5	1.426	1.441
1–3	1.417	1.403	2–4	1.419	1.456
1–4	1.390	1.492	3–5	1.396	
	2a	2	1–4	1.422	1.397
2–5	1.422	1.424	3–6	1.422	1.497
2–4	1.431	1.445	1–6	1.369	1.483
3–4	1.408	1.415		5a	5
1–4	1.419	1.392	5–8	1.423	1.435
1–6	1.390	1.493	2–8	1.420	1.423
			2–7	1.423	1.442
			2–6	1.429	1.449
			1–6	1.429	1.388
			1–9	1.368	1.485
			3–9	1.423	1.498
			3–7	1.423	1.389
			4–6	1.403	1.410

eigenvectors of the Hückel matrix, three are directly obtained as the allyl nonbonding MOs associated to each fragment, the fourth one is symmetrical and centered on the central atom, as pictured in Scheme 6, left and right, respectively, prior to amplitude normalization.

This molecule may be seen as four spins in ferromagnetic interactions with negative J^{eff} between the central and external spins. Solutions of this Heisenberg Hamiltonian are easily calculated: Above the quintet ground state, there are three triplet states, two of them degenerate at energy $-J^{\text{eff}}$, and one symmetrical at energy $-4J^{\text{eff}}$, the first singlet state lying at $-3J^{\text{eff}}$ above.

The spacing regularities in relative energies of these low-lying states calculated from Heisenberg Hamiltonian could be a clue for a simplified view of **1**, as a four-site magnetic skeleton of trimethylene-methane type (Scheme 7). This is supported by the nature of nonbonding orbitals, three of them peripheral and non-interacting, the fourth one at the center. In this scheme, the only interaction at work is the

Table 1. Summary of calculated vertical transition energies (in eV), with spin-operator characteristics for the UDFT solutions.

S_z	$\langle S^2 \rangle_{\text{exp}}$	UDFT				Heisenberg	Correlated ab initio					
		$\langle S^2 \rangle_{\text{calcd}}$	raw	corrected	CASPT2		CASCI	CAS+S	DDCI2	DDCI		
1	0	2.00	2.03	0.63		singlet	1.03	1.35	2.24	1.09	1.00	1.62
	1	3.00	3.05	0.31	0.41	triplet	0.33	0.57	0.78	0.40	0.36	0.41
	2	6.00	6.09	0.0	0.0	quintet (${}^5A_2'$)	0.0	0.0	0.0	0.0	0.0	0.0
2a	0	1.00	1.04	0.29	0.59	singlet	0.82	0.30	1.60	0.81	0.71	0.76
	1	2.00	2.11	0.0	0.0	triplet (${}^3A_1'$)	0.0	0.0	0.0	0.0	0.0	0.0
	1/2	2.75	2.79	0.87		doublet	0.95	1.18	2.00	1.15	1.01	
2	3/2	4.75	4.85	0.49	0.62	quartet	0.43	0.84	0.96	0.54	0.49	
	5/2	8.75	8.93	0.0	0.0	sextet (${}^6A_2''$)	0.0	0.0	0.0	0.0	0.0	
	0	3.00	3.09	0.77		singlet	0.90	1.09	1.25	0.93		
4	1	4.00	4.10	0.52		triplet	0.51	0.59	0.89	0.58	0.52	
	2	7.00	7.14	0.24	0.30	quintet	0.22	0.28	0.41	0.26	0.23	
	3	12.00	12.17	0.0	0.0	septet (${}^7A_2'$)	0.0	0.0	0.0	0.0	0.0	

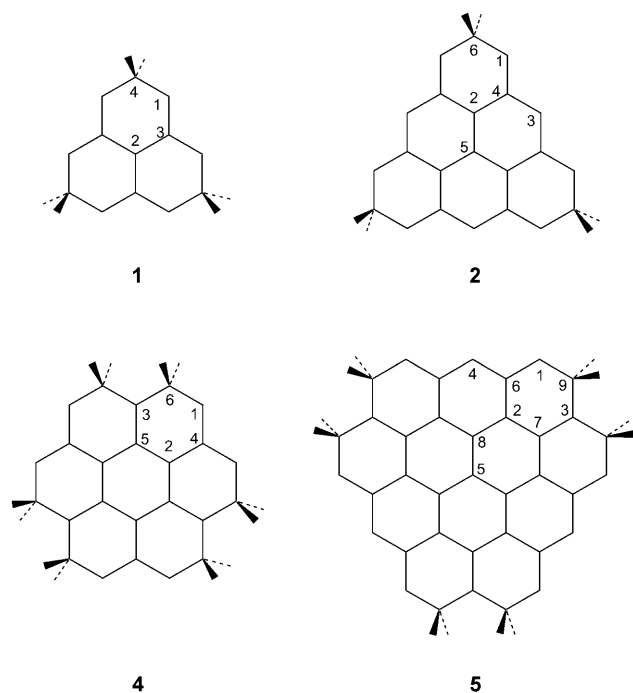
Table 3. Calculated spin densities on carbon atoms for high-spin states (see Scheme 5 for labeling).

Method	Center	1a	1	2a	2	4	5a	5
Hückel	1	0.17	0.60	0.18	0.53	0.58	0.06	0.52
	2	0.0	0.40	0.06	0.25	0.33	0.01	0.22
	3	0.0	0.0	0.24	0.36	0.51	0.06	0.45
	4	0.0		0.0	0.0	0.0	0.12	0.35
	5			0.0	0.0	0.0	0.0	0.17
	6			0.0			0.0	0.0
	7						0.0	0.0
	8						0.0	0.0
	9						0.0	0.0
Heisenberg	1	0.37	0.80	0.20	0.73	0.79		
	2	0.35	0.75	0.20	0.68	0.72		
	3	-0.28	-0.51	0.24	0.71	0.73		
	4	-0.25		-0.07	-0.50	-0.50		
	5			-0.03	-0.56	-0.52		
	6			-0.04				
UDFT	1	0.30	0.75	0.34	0.67	0.73	0.13	0.66
	2	0.06	0.62	0.18	0.50	0.58	0.07	0.47
	3	-0.13	-0.30	0.39	0.57	0.61	0.15	0.55
	4	-0.14	-0.13	-0.16	-0.28	-0.30	0.23	0.55
	5			-0.14	-0.30	-0.31	0.15	0.46
	6			-0.17	-0.12	-0.13	-0.08	-0.27
	7						-0.07	-0.27
	8						-0.08	-0.30
	9						-0.09	-0.11
CASCI	1	0.16	0.54	0.18	0.44	0.53		
	2	0.00	0.45	0.04	0.27	0.43		
	3	0.01	0.04	0.22	0.37	0.31		
	4	0.01	0.02	0.01	0.03	0.04		
	5			0.00	0.02	0.03		
	6			0.01	0.02	0.02		
CAS+S	1	0.28	0.71	0.31	0.59	0.67		
	2	0.04	0.63	0.12	0.43	0.57		
	3	-0.10	-0.23	0.36	0.51	0.50		
	4	-0.12	-0.10	-0.12	-0.17	-0.19		
	5			-0.09	-0.18	-0.19		
	6			-0.13	-0.08	-0.07		
DDCI	1	0.21	0.62	0.23	0.50			
	2	0.00	0.54	0.07	0.34			
	3	-0.04	-0.09	0.27	0.44			
	4	-0.04	-0.05	-0.04	-0.05			
	5			-0.02	-0.06			
	6			-0.04	-0.03			
odd-electron number								
total		1	4	2	5	6	1	7
per site		0.08	0.40	0.09	0.26	0.33	0.03	0.23

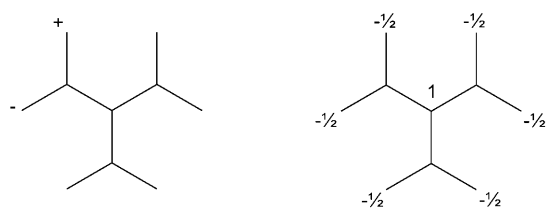
ferromagnetic coupling J^{eff} between the center and the periphery. Confronting the six eigenenergies calculated in this 4-site simplified set to the six lowest eigenenergies of the 10-site original set actually shows a good agreement. The Heisenberg calculations on the full 10-site system locate the low-lying states of **1** at 0.33, 1.03, and 1.33 eV, a degenerate triplet, a degenerate singlet, and a triplet, above the quintet ground state, respectively. In the simplified 4-site model, these values come out as J^{eff} , $3J^{\text{eff}}$, and $4J^{\text{eff}}$ respectively, which, when setting J^{eff} to -0.335 eV, correspond to 0.33, 1.01, and 1.34 eV, respectively. This illustrates how prior identification of semilocalized spins in doublet ground-state

fragments can simplify a magnetic picture, in the spirit of real space renormalization group (RSRG).^[67–69]

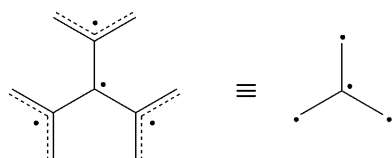
The UDFT lowest solution is actually obtained for $S_z=2$, corresponding to optimized bond lengths and spin densities reported in Tables 1 and 2, respectively. This four-electron–four-orbital system gives rise to triplet and singlet excited states. The $S_z=1$ solution is calculated at 0.41 eV above the quintet state, and the $S_z=0$ solution is calculated at 0.63 eV above the quintet state. For the former gap, the ab initio CI approaches confirm this value (0.41 eV at the DDCI level). For the transition toward the singlet state, Heisenberg, CAS+S and DDCI2 levels suggest a value around 1 eV,



Scheme 5. Numbering scheme used in Tables 1–3, also applying to the **a**-suffixed compounds.



Scheme 6.



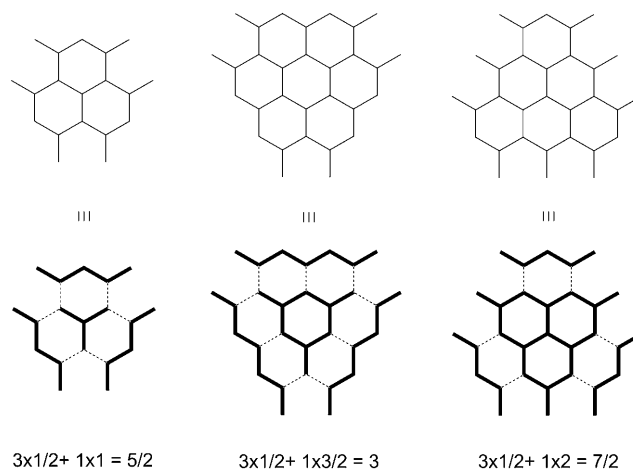
Scheme 7.

whereas the reference DDCI value comes out larger, at 1.62 eV. The three approaches therefore agree on both ground-state spin multiplicity and transition energies toward the first low-lying state of lower spin multiplicity.

Six-ring structures: The fully conjugated triangular structure, **2a**, sometimes called triangulene,^[39] is expected to have a triplet ground state, as the Hückel Hamiltonian gives two nonbonding orbitals, the shape of which may immediately be assigned D_{2h} symmetry. The resulting spin densities can be compared with those predicted by the Heisenberg treatment and the $S_z=1$ UDFT calculations (Table 3). Not unex-

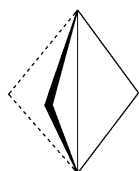
pectedly, the geometry predicted by this calculation indicates some relationship between the length of a given bond, and its spin alternation, defined as the product of spin densities on the two concerned atoms. We will go back to this point later on. The UDFT calculation for $S_z=0$ gives an energy 0.29 eV higher than that associated to $S_z=1$, confirming the nature of the ground state. Approximate spin decontamination raises this value to 0.59 eV, a gap not too much different from that obtained from the best ab initio DDCI calculation (0.76 eV), or the crude Heisenberg calculation 0.82 eV.

Saturation of the three corner carbons leads to **2**, a molecule with five unpaired electrons, of sextet ground-state spin multiplicity, the five nonbonding orbitals again being predicted by Hückel theory. Actually, three of them may be defined from sets of peripheral conjugated atoms identifiable to the nonbonding orbitals of pentadienyl radicals (see Scheme 8, left). The two remaining orthogonal nonbonding



Scheme 8. Picturing **2b**, **3b**, and **5b** as three peripheral polyenyl monoradicals interacting with a central polyradical kernel. Total-spin decomposition is made explicit.

orbitals are centered in the molecular core region, and can be seen as the nonbonding orbitals of a trimethylene-methane moiety, with outward delocalization tails. Interestingly, this evokes a d^5 metallic center in octahedral environment, with $3t_{2g}$ and $2e_g$ degenerate orbitals. Changing the electroaffinity of the central atom would further split here the central/periphery energy difference, in the same way crystal field plays with t_{2g}/e_g energy splitting in coordination chemistry. Scheme 8 illustrates how the center/periphery breaking down holds for all our compounds with three-fold symmetry, in which peripheral polyenyl monoradicals are associated to different central parts. Here again, semilocalization of nonbonding orbitals suggests a renormalized vision in terms of five $S_z=1/2$ spins located on the vertices of a trigonal bipyramid. The three in-plane vertices do not interact directly, but are ferromagnetically coupled with the two axial ones, which in turn are coupled to each other (Scheme 9).

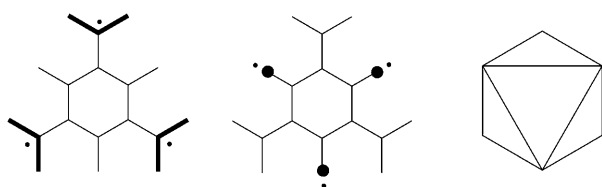


Scheme 9.

As expected, the UDFT calculation for $S_z=5/2$ gives the lowest-energy solution—the $S_z=3/2$ solution is 0.49 eV above—and spin decontamination has only a moderate effect (0.62 eV). The spatial symmetry of the wavefunction is broken, as the lowest quartet state is de-

generate in the D_{3h} geometry. Geometry relaxation does not significantly lower the energy of the corresponding determinant. The ab initio CI and Heisenberg Hamiltonian calculations confirm the order of magnitude of the sextet-to-quartet vertical excitation energy (0.49 eV and 0.43 eV, respectively). The UDFT calculation of the lowest $S_z=1/2$ solution locates the doublet state above 0.87 eV (Equation (4) is here no longer relevant for spin decontamination), a value in line with both Heisenberg and DDCI results, around 1 eV. For this example, let us have a look on how the spin-density distributions of Table 3 are predicted by the various methods. If they agree on locating major spin carriers, they differ on the other centers, and on the amplitudes of the contrasts. Negative spin densities, linked to spin polarization, are of course absent in Hückel and CASCI calculations, which give similar values. Including spin polarization creates negative densities on minor-color atoms, while increasing the positive densities on the other set. In this way, it tends towards the spin distribution of a fully-alternant VB single determinant. Owing to the absence of ionic components in the wavefunction, Heisenberg description overestimates the contrasts. The UDFT spin distribution appears as intermediate between the Heisenberg and the extended CI descriptions, which tempers the amplitudes.

Septet ground state from coronene: Higher multiplicity can be obtained from closed-shell coronene **4a** by transforming six peripheral atoms of the same color into sp^3 carbons. The resulting conjugated system **4** implies 18 atoms and bears six unpaired electrons. It can be seen as a radialene ring, in which three exocyclic CC bonds in *meta* bear two methylene groups, or as an hexa-radical structure, with a central benzene ring bearing alternatively methylene and allyl groups, **4b**. This last view is closer to the Hückel solution, giving six nonbonding orbitals. Three of them are localized on the peripheral allyl fragments, whereas the three other ones have their largest amplitude on the peripheral methylene carbons, with important delocalization tails (Scheme 10, left and middle). This picture suggests viewing the system as unpaired electrons semilocalized in distinct molecular regions



Scheme 10.

interacting with one another in a ferromagnetic way through the central benzene ring. The 18-site molecule is then reduced to a hexagon of alternating allyl/methylene magnetic entities. The equivalent simplified frame would be here a set of two intricate triangles with ferromagnetic-coupling links, as in Scheme 10 right. Again, this transformation from 18 sites to six pseudo-sites is in RSRG spirit, and the effective magnetic interactions between the latter would deserve to be determined from the exact spectrum.

The UDFT calculations confirm the septuplet spin multiplicity of the ground state. Increasing the size of the system and the number of unpaired electrons should result in lesser excitation energy toward the state of immediate lower multiplicity. Actually the excitation energy to the lowest quintet is calculated to be around 0.23 eV, with a good agreement between the various methods (see Table 1)—a quantity much larger than kT at room temperature (0.026 eV at 25°C). Given such energy gaps between lowest states, the molecule can definitely be seen as a high-spin moiety.

Twelve-ring structures: On systems **5a** and **5**, only UDFT calculations could be performed. If **5** derives from **5b**, the higher analogue of **2b**, note that **5a** is not the higher analog of **2a**. Both **5b** and **5** bear seven unpaired electrons, whose spin densities are given in Table 3. The first excited state of **5**, a sextet, is located at 0.45 eV, amended to 0.54 eV after proper treatment from $\langle S_{UHF}^2 \rangle$, calculated at 9.97 instead of 8.75, making **5** a sure high-spin candidate. Returning to the geometrical trend analyses, from Tables 2 and 3, it is clear that concentrating parallel spins on (or rising the probability of triplet arrangement between) adjacent atoms significantly increases the corresponding bond length, as mentioned above. Further margin reduction and quantification of this relationship, however, turned out to be poorly effective. On the other hand, gathering all C–C bond lengths in high-spin ground states offers interesting trends. In fully conjugated **1a**, **2a**, **4a**, and **5a**, the C–C bond lengths are lie around the typical aromatic value (1.37–1.43 Å). After the procedure of corner saturation, the C–C bond lengths in **1**, **2**, **4**, and **5** now splits, with a $C(sp^2)$ – $C(sp^3)$ subset tending towards typical single-bond values, while the remaining conjugated bonds range between aromatic bonds (1.39 Å) and single bonds in conjugated hydrocarbon (1.45 Å).

Conclusion

Obtained from fused aromatic hydrocarbons, the molecular systems proposed in this work have a ground state of high-spin multiplicity, and are very compact. The conceptual guide to conceive such magnetic architectures is rather simple, and rests on the coloring partition of atoms over alternant graphs. From pure polycyclic aromatic systems, the higher density of unpaired and parallel electrons can be obtained by chemical saturation of carbons of a specific color, which subtracts them from the conjugated frame. These structures can hardly be considered as polyradicals in the

usual organic-chemistry sense, as unpaired electrons here occupy a same portion of space. Although they may be localized to some extent, their domains still overlap. Yet, despite this overlap, their coupling is ferromagnetic, as a result of orthogonality constraints applying to the lower-energy closed-shell orbitals. The overall spin multiplicity definitely appears as a collective property.

The present work has made use of different fundamental pictures pertaining to the panoply of quantum chemistry. We have invoked the Hückel model to directly produce semilocalized nonbonding MOs. The qualitative arguments applied to guess the ground-state spin multiplicity belong to the valence-bond way of thinking. The related Heisenberg Hamiltonian provides a reliable spectrum of states associated with a same space part and different spin multiplicities. The UDFT computational tool gives reliable geometries for the ground state and a rough estimate of excitation energies to states of lower multiplicity. The ab initio CI calculations furnish a reliable excitation spectrum. Selective and discerning use of these tools, some of them now forgotten in most textbooks, exploits the richness of the cultural background of quantum chemistry and the persisting relevance of its historical apportionments.

As we subsequently intend to address 2D space covering, the compounds chosen here for illustrating our building strategy have a suitable threefold symmetry. However, this is in no way a requirement, as surface filling can proceed from fourfold or sixfold symmetries as well. Taken separately, such building blocks can be planned to be adsorbed on surfaces,^[70] but for our part we will study in a next work how to couple them straight into periodic ferromagnetic arrangements.

Appendix

Evaluation of ferromagnetic coupling from the amplitudes of Hückel nonbonding orbitals: The nonbonding molecular orbitals (NBO) given by the Hückel Hamiltonian may be localized on different domains of the molecule, with spatial overlap between these domains. Given two NBOs ϕ_i and ϕ_j , their expansion on the atomic $2p_z$ orbitals p, q, \dots , is written as Equation (6):

$$|\phi_i\rangle = \sum_p C_{ip} |p\rangle \quad (6)$$

The direct exchange integral between ϕ_i and ϕ_j , leads to Equation (7):

$$K_{ij} = \langle \phi_i(1)\phi_j(2) | \frac{1}{r_{12}} | \phi_j(1)\phi_i(2) \rangle \quad (7)$$

This may be calculated in terms of bielectronic integrals between atomic orbitals. If the bielectronic repulsion operator is the bielectronic part of the Hubbard Hamiltonian, that is, restricted to on-site interactions, then Equation (8):

$$\langle p(1)q(2) | \frac{1}{r_{12}} | r(1)s(2) \rangle = U\delta(p,r)\delta(q,s)\delta(p,q) \quad (8)$$

Then the exchange integral K_{ij} in Equation (9):

$$K_{ij} = U \sum_p C_{ip}^2 C_{jp}^2 \quad (9)$$

From this expression, the exchange keeps a zero value if the domains of definition of the two NBOs do not share any atomic orbital. This is why we may assume that unpaired electrons do not interact in our peripheral semilocalized NBOs.

Evaluation of exchange integrals between peripheral and central NBOs is straightforward, as long as their amplitudes are known. We thus obtained the following results for the above-addressed compounds. In **1**, the exchanges are of the same type, which concerns the interaction between the central NBO and peripheral ones, and $K_{ij} = U/10$. Taking $U = 3$ eV, then $K_{ij} = 0.3$ eV, which coincides with the value of J^{eff} fitting the calculated low-energy spectrum of the whole molecule. Compound **2** presents two types of exchanges (cf. Scheme 9). That between one peripheral NBO and the central ones is calculated at $J_1 = 2/45 U$. That between the two central NBOs is larger since they are defined in the same region of space: $J_2 = 9/75 U$, just above the value of J^{eff} in **1**. In compound **4**, the exchange integral between internal sites is rather large, ($J_2 = U/11$), whereas that between a peripheral allylic site and its closer central ones is smaller ($J_1 = U/32$). The interaction between a peripheral site and its remote internal site is even smaller, $J_1 = U/51$, justifying its neglect in the graph of Scheme 10.

Acknowledgements

We thank Prof. Nathalie Guihéry and Dr. Thomas Guillon for helpful discussions and computational assistance.

- [1] *Magnetic Molecular Materials* (Eds.: D. Gatteschi, O. Kahn, J. S. Miller, F. Palacio), Kluwer, Dordrecht, **1991**.
- [2] O. Kahn, *Molecular Magnetism*, VCH, Weinheim, **1993**.
- [3] D. Gatteschi, *Adv. Mater.* **1994**, *6*, 635.
- [4] J. S. Miller, A. J. Epstein, *Angew. Chem.* **1994**, *106*, 399; *Angew. Chem. Int. Ed. Engl.* **1994**, *33*, 385.
- [5] O. Kahn, *Acc. Chem. Res.* **2000**, *33*, 647.
- [6] R. Georges, J. J. Borrás-Almenar, E. Coronado, J. Curély, M. Drillon in *Magnetism: Molecules to Materials, Vol. 1* (Eds.: J. S. Miller, M. Drillon), Wiley-VCH, Weinheim, **2001**, Chapter 1, p. 1.
- [7] M. Verdager, *Polyhedron* **2004**, *23*, 1115.
- [8] J. Souletie, P. Rabu, M. Drillon in *Magnetism: Molecules to Materials, Vol. 5* (Eds.: J. S. Miller, M. Drillon), Wiley-VCH, Weinheim, **2005**, Chapter 10, p. 347.
- [9] H.-Q. Dingh, *J. Phys. Condens. Matter* **1990**, *2*, 7979.
- [10] T. Barnes, *Int. J. Mod. Phys. A* **1991**, *2*, 659.
- [11] K. Ueda, T. Moriya, Y. Takahashi, *J. Phys. Chem. Solids* **1992**, *53*, 1515.
- [12] A. M. Allegra, H. Matsumoto, S. Odashima, *J. Phys. Condens. Matter* **1996**, *8*, 4411.
- [13] E. L. Nagaev, *Phys. Rep.* **2001**, *346*, 387.
- [14] *Colossal Magnetoresistive Oxides* (Ed.: Y. Tokura), Gordon and Breach, Amsterdam, **2000**.
- [15] T. Kimura, Y. Tokura, *Lect. Notes Phys.* **2002**, *595*, 361.
- [16] M. Verdager, G. S. Girolami in *Magnetism: Molecules to Materials, Vol. 5* (Eds.: J. S. Miller, M. Drillon), Wiley-VCH, Weinheim, **2005**, Chapter 9, p. 283.
- [17] J. S. Miller, *Pramana* **2006**, *67*, 1.
- [18] J. S. Miller in *Engineering of Crystalline Materials Properties* (Eds.: J. J. Novoa, D. Braga, L. Addadi), Springer, Amsterdam, **2008**, p. 291.
- [19] Landolt-Börnstein, *Magnetic Properties of Free Radicals, Group II: Molecules and Radicals, Vol. 26, Supplement D: Nitroxide Radicals and Nitroxide Based High-Spin Systems*, Springer, Heidelberg, **2005**.
- [20] C. Train, L. Norel, M. Baumgarten, *Coord. Chem. Rev.* **2009**, *253*, 2342.
- [21] *Carbon-based Magnetism: An Overview of the Magnetism of Metal-free Carbon-based Compounds and Materials* (Eds.: T. L. Makarova, F. Palacio), Elsevier, Amsterdam, **2006**.
- [22] H. Ma, C. Liu, C. Zhang, Y. Jiang, *J. Phys. Chem. A* **2007**, *111*, 9471.

- [23] D. Gatteschi, L. Bogani, A. Cornia, M. Mannini, L. Sorace, R. Sessoli, *Solid State Sci.* **2008**, *10*, 1701.
- [24] A. Rajca, *Chem. Rev.* **1994**, *94*, 871.
- [25] A. Rajca, J. Wongsriratanakul, S. Rajca, *J. Am. Chem. Soc.* **1997**, *119*, 11674.
- [26] A. Rajca, S. Rajca, J. Wongsriratanakul, *J. Am. Chem. Soc.* **1999**, *121*, 6308.
- [27] A. Rajca, J. Wongsriratanakul, S. Rajca, *Science* **2001**, *294*, 1503.
- [28] A. Rajca, J. Wongsriratanakul, S. Rajca, R. L. Cerny, *Chem. Eur. J.* **2004**, *10*, 3144.
- [29] A. Rajca, J. Wongsriratanakul, S. Rajca, *J. Am. Chem. Soc.* **2004**, *126*, 6608.
- [30] S. Rajca, A. Rajca, J. Wongsriratanakul, P. Butler, S.-M. Choi, *J. Am. Chem. Soc.* **2004**, *126*, 6972.
- [31] M. Nakano, R. Kishi, S. Ohta, H. Takahashi, T. Kubo, K. Kamada, K. Ohta, E. Botek, B. Champagne, *Phys. Rev. Lett.* **2007**, *99*, 033001; K. Kamada, K. Ohta, T. Kubo, A. Shimizu, Y. Morita, K. Nakasuji, R. Kishi, S. Ohta, S. Furukawa, H. Takahashi, M. Nakano, *Angew. Chem.* **2007**, *119*, 3614; *Angew. Chem. Int. Ed.* **2007**, *46*, 3544.
- [32] For previous semiempirical explorations, see: S. Li, J. Ma, Y. Jiang, *J. Phys. Chem. A* **1997**, *101*, 5567.
- [33] J.-P. Malrieu, D. Maynau, *J. Am. Chem. Soc.* **1982**, *104*, 3021.
- [34] D. Maynau, J.-P. Malrieu, *J. Am. Chem. Soc.* **1982**, *104*, 3029.
- [35] D. Maynau, M. Said, J.-P. Malrieu, *J. Am. Chem. Soc.* **1983**, *105*, 5244.
- [36] M. Said, D. Maynau, J.-P. Malrieu, M. A. Garcia-Bach, *J. Am. Chem. Soc.* **1984**, *106*, 571.
- [37] M. Said, D. Maynau, J.-P. Malrieu, *J. Am. Chem. Soc.* **1984**, *106*, 580.
- [38] F. Bernardi, M. Olivucci, M. A. Robb, *J. Am. Chem. Soc.* **1992**, *114*, 1606.
- [39] M. J. Bearpark, M. A. Robb, M. Bernardi, M. Olivucci, *Chem. Phys. Lett.* **1994**, *217*, 513.
- [40] M. J. Bearpark, F. Bernardi, M. Olivucci, M. A. Robb, *J. Phys. Chem. A* **1997**, *101*, 8395.
- [41] M. J. Bearpark, M. Boggio-Pasqua, *Theor. Chem. Acc.* **2003**, *110*, 105.
- [42] M. Garavelli, F. Ruggeri, F. Ogliaro, M. J. Bearpark, F. Bernardi, M. Olivucci, M. A. Robb, *J. Comput. Chem.* **2003**, *24*, 1357.
- [43] M. J. Bearpark, M. Boggio-Pasqua, M. A. Robb, F. Ogliaro, *Theor. Chem. Acc.* **2006**, *116*, 670.
- [44] M. J. Bearpark, F. Ogliaro, T. Vreven, M. Boggio-Pasqua, M. J. Frisch, S. M. Larkin, M. Morrison, M. A. Robb, *J. Photochem. Photobiol. A* **2007**, *190*, 207.
- [45] A. A. Ovchinnikov, *Theor. Chim. Acta* **1978**, *47*, 297.
- [46] On violations of Hund's rule in non-Kekulé hydrocarbons in general, see: W. T. Borden, H. Iwamura, J. A. Berson, *Acc. Chem. Res.* **1994**, *27*, 109.
- [47] Of course, the rule can be violated for twisted geometries; see, for instance: S. Fang, M.-S. Lee, D. A. Hrovat, W. T. Borden, *J. Am. Chem. Soc.* **1995**, *117*, 6727.
- [48] N. Guihéry, D. Maynau, J.-P. Malrieu, *New J. Chem.* **1998**, *22*, 281.
- [49] D. R. McMasters, J. Wirz, G. J. Snyder, *J. Am. Chem. Soc.* **1997**, *119*, 8568.
- [50] J. M. Zoellner, R. W. Zoellner, *J. Mol. Struct.* **2008**, *871–892*, 50.
- [51] E. Kariv-Miller, R. I. Pacut, *Tetrahedron* **1986**, *42*, 2185.
- [52] E. Kariv-Miller, R. I. Pacut, G. K. Lehman, *Top. Curr. Chem.* **1988**, *148*, 97.
- [53] W. Zhizhong, C. Breakman-Danheux, S. Boué, A. Fontana, *Fuel Process. Technol.* **1990**, *25*, 251.
- [54] M. W. Bedell, C. W. Curtis, *Energy Fuels* **1991**, *5*, 469.
- [55] E. G. Palfy, P. Starzewsky, A. Labani, A. Fontana, *J. Appl. Electrochem.* **1994**, *24*, 337.
- [56] S. Anowski, J. Voss, *J. Prakt. Chem./Chem.-Ztg.* **1996**, *338*, 337.
- [57] The ab initio calculations at correlated-level were done using ANO-RCC atomic basis sets. For carbon atom, a 14s9p4d primitive set is contracted to 3s2p1d (B. O. Roos, R. Lindh, P.-A. Malmqvist, V. Veryazov, P.-O. Widmark, *J. Phys. Chem. A* **2005**, *109*, 2851); for hydrogen atom a 8s primitive set is contracted to 2s (P.-O. Widmark, P.-A. Malmqvist, B. O. Roos, *Theor. Chim. Acta* **1990**, *77*, 291).
- [58] K. Andersson, P.-A. Malmqvist, B. O. Roos, A. J. Sadlej, K. Wolinski, *J. Phys. Chem.* **1990**, *94*, 5483; K. Andersson, P.-A. Malmqvist, B. O. Roos, *J. Chem. Phys.* **1992**, *96*, 1218.
- [59] J. Miralles, J.-P. Daudey, R. Caballol, *Chem. Phys. Lett.* **1992**, *198*, 555; J. Miralles, O. Castell, R. Caballol, J.-P. Malrieu, *Chem. Phys.* **1993**, *172*, 33.
- [60] The UDFT calculations were performed with the Gaussian 03 quantum chemistry package (Gaussian 03, Revision B.05, M. J. Frisch, G. W. Trucks, H. B. Schlegel, G. E. Scuseria, M. A. Robb, J. R. Cheeseman, J. A. Montgomery, Jr., T. Vreven, K. N. Kudin, J. C. Burant, J. M. Millam, S. S. Iyengar, J. Tomasi, V. Barone, B. Mennucci, M. Cossi, G. Scalmani, N. Rega, G. A. Petersson, H. Nakatsuji, M. Hada, M. Ehara, K. Toyota, R. Fukuda, J. Hasegawa, M. Ishida, T. Nakajima, Y. Honda, O. Kitao, H. Nakai, M. Klene, X. Li, J. E. Knox, H. P. Hratchian, J. B. Cross, V. Bakken, C. Adamo, J. Jaramillo, R. Gomperts, R. E. Stratmann, O. Yazyev, A. J. Austin, R. Cammi, C. Pomelli, J. W. Ochterski, P. Y. Ayala, K. Morokuma, G. A. Voth, P. Salvador, J. J. Dannenberg, V. G. Zakrzewski, S. Dapprich, A. D. Daniels, M. C. Strain, O. Farkas, D. K. Malick, A. D. Rabuck, K. Raghavachari, J. B. Foresman, J. V. Ortiz, Q. Cui, A. G. Baboul, S. Clifford, J. Cioslowski, B. B. Stefanov, G. Liu, A. Liashenko, P. Piskorz, I. Komaromi, R. L. Martin, D. J. Fox, T. Keith, M. A. Al-Laham, C. Y. Peng, A. Nanayakkara, M. Challacombe, P. M. W. Gill, B. Johnson, W. Chen, M. W. Wong, C. Gonzalez, J. A. Pople, Gaussian, Inc., Wallingford CT, **2004**) with B3LYP hybrid functional, using 6-311G** internal basis sets. Geometry optimizations on high-spin states were carried on up to energy gradients around 10⁻⁴ au in worst cases.
- [61] L. Noodleman, *J. Chem. Phys.* **1981**, *74*, 5737.
- [62] C. J. Calzado, J. Cabrero, J.-P. Malrieu, R. Caballol, *J. Chem. Phys.* **2002**, *116*, 2728; C. J. Calzado, J. Cabrero, J.-P. Malrieu, R. Caballol, *J. Chem. Phys.* **2002**, *116*, 3985.
- [63] L. V. Slipchenko, A. I. Krylov, *J. Chem. Phys.* **2002**, *117*, 4694.
- [64] P. G. Wenthold, J. Hu, R. R. Squires, W. C. Lineberger, *J. Am. Chem. Soc.* **1996**, *118*, 475.
- [65] T. Wang, A. I. Krylov, *J. Chem. Phys.* **2005**, *123*, 104304.
- [66] P. G. Wenthold, J. B. Kim, W. C. Lineberger, *J. Am. Chem. Soc.* **1997**, *119*, 1354.
- [67] K. G. Wilson, *Rev. Mod. Phys.* **1975**, *47*, 773.
- [68] C. J. Morningstar, M. Weinstein, *Phys. Rev. D* **1996**, *54*, 4131.
- [69] J.-P. Malrieu, N. Guihéry, *Phys. Rev. B* **2001**, *63*, 085110.
- [70] N. Tyutyulkov, F. Dietz, K. Müllen, *Chem. Phys. Lett.* **2000**, *331*, 465.

Received: January 8, 2010
Published online: June 22, 2010